Vibrational properties of Ga-stabilized δ-Pu by extended x-ray absorption fine structure

P. G. Allen,* A. L. Henderson, and E. R. Sylwester
Seaborg Institute for Transactinium Science, Lawrence Livermore National Laboratory, P.O. Box 808, Livermore, California 94551

P. E. A. Turchi, T. H. Shen, and G. F. Gallegos
Materials Science and Technology Division, Lawrence Livermore National Laboratory, P.O. Box 808, Livermore, California 94551

C. H. Booth
Chemical Sciences Division, Lawrence Berkeley National Laboratory, Berkeley, California 94720
(Received 7 December 2001; revised manuscript received 14 February 2002; published 5 June 2002)

Temperature-dependent extended x-ray absorption fine structure (EXAFS) spectra were measured for a 3.3 at.% Ga stabilized Pu alloy over the range $T=20-300$ K. EXAFS data were acquired at both the Ga *K* edge and the Pu L_{III} edge. Curve fits were performed to the first shell interactions to obtain pair-distance distribution widths σ as a function of temperature. The temperature dependence of $\sigma(T)$ was accurately modeled using a correlated-Debye model for the lattice vibrational properties, suggesting Debye-like behavior in this material. Using this formalism, we obtain pair-specific correlated-Debye temperatures Θ_{cD}, of 110.7 $\pm$1.7 K and 202.6$\pm$3.7 K, for the Pu-Pu and Ga-Pu pairs, respectively. The result for the Pu-Θ_{cD} value compares well with previous vibrational studies on δ-Pu. In addition, our results represent the first unambiguous determination of Ga-specific vibrational properties in PuGa alloys, i.e, Θ_{cD} for the Ga-Pu pair. Because the Debye temperature can be related to a measure of the lattice stiffness, these results indicate the Ga-Pu bonds are significantly stronger than the Pu-Pu bonds. This effect has important implications for lattice stabilization mechanisms in these alloys.

DOI: 10.1103/PhysRevB.65.214107 PACS number(s): 61.10.Ht, 61.66.Dk, 63.20.Dj

I. INTRODUCTION

Plutonium in its elemental form presents a complicated picture of phase stability.[1] Indeed, Pu may adopt one of six crystallographically different phases (α, β, γ, δ, δ', and ϵ) upon heating from room temperature to its melting point of 913 K. This complex phase behavior has been explained, in part, by the behavior of the Pu $5f$ orbitals which fluctuate between itinerant and localized behavior. In this heuristic framework, elemental Pu represents the transition point along the actinide series from the delocalized electronic nature of the early actinides (Ac-Np) to localized, lanthanide-like *f*-orbital character observed for the heavier actinides.[2] Theoretical calculations currently support the hypothesis that the $5f$ orbitals are delocalized for elements lighter than Pu in the actinide series and localized for those heavier than Pu.[3] This view of the relationship between electronic and crystallographic structure is reinforced by comparing the complex phase behavior and structures observed for pure U, Np, and Pu metals as opposed to the relatively simple structures observed for the elements Am and beyond.

The structural and electronic relationships that exist between the α and δ phases have received much attention due to some unusual observations. Pure face-centered cubic (fcc) δ-Pu is stable from 593 to 736 K, and exhibits a 25% increase in volume relative to that of the ground state phase,[1] monoclinic α-Pu. However, it is well known that the fcc structure can be stabilized down to ambient temperature by the addition of small amounts ($\sim$3–9 at.%) of alloying elements such as Al, Ga, In, Sc, and Ce.[4] However, at lower impurity atom concentrations, the δ phase converts directly to the α form upon cooling, possibly through a Martensitic phase transformation.[5,6]

Other than a tendency to form trivalent cations, relatively little is known about the mechanism of these so-called "δ stabilizers."[7,8] Band structure studies have suggested that Al, Ga, and Sc impurities diffuse the $5f$ bands, thereby removing their involvement in bonding and leading to the stability of a more common, *d*-bonded transition metal-like phase.[9] Becker *et al.* have employed an *ab initio* LDA approach to study the lattice relaxation in a $Pu_{31}Ga$ supercell cluster, and find evidence of a lattice contraction around the Ga site which relaxes the bonding constraints for the neighboring Pu atoms.[10] Other theoretical works[11] point to a substantial level of $5f$ localization in the δ phase[12] and have speculated on a Kondo-like model for the involvement of the $5f$ electrons.[13]

Analysis of the vibrational properties in these materials is also important for understanding δ-phase stablization. Unfortunately, measurement of the phonon dispersion using conventional inelastic neutron scattering techniques is troublesome given the difficulty in growing high-quality single crystals. An alternative approach is to evaluate the Debye temperature Θ_D using various structural techniques. Ledbetter *et al.*[14] employed ultrasonic wave measurements of elastic constants for 3.3 at.% Ga δ-Pu and calculated a $\Theta_D$value of 115 K. The thermal behavior of 5.0 at.% Al δ-Pu was studied by temperature-dependent neutron powder diffraction[15] yielding a similarly low value of $\Theta_D=132$ K. More recently, Lynn *et al.*[16] studied a 3.6 at.% Ga δ-Pu sample using neutron-resonance Doppler spectroscopy, a technique that can determine element specific values for Θ_D. The experiments determined a Pu-specific value of $\Theta_D=127$ K, and assigned a Ga specific value of $\Theta_D=255$ K,

although with relatively large errors (± 22 K). As a test of the Debye model, one can check the assumption of equal force constants for the Pu and Ga sites by comparing the Ga-Θ_D to the $\sqrt{m_{\mathrm{Pu}}/m_{\mathrm{Ga}}}$ weighted value of 236 K derived from the Pu-Θ_D value. Thus, this comparison does not exclude the possibility that the Ga atoms experience a stiffer force field compared with the Pu atoms.

In this article, we present temperature dependent EXAFS (extended x-ray absorption fine-structure) spectroscopic results for 3.3 at.% Ga δ-Pu as a means of discerning differences in the vibrational character of the Ga and Pu sites. Previously, EXAFS studies on Ga stabilized δ-Pu have focused on isothermal measurements at either the Ga *K* or the Pu L_{III} edges, and have revealed some important effects.[17–19] In general, these studies indicate that the Ga atoms reside in their expected fcc lattice positions although there is an appreciable lattice contraction observed for the Ga-Pu bonds ($\sim$3–4 %). Surprisingly, the contraction in Ga-Pu bonds is significantly larger than the collapse calculated theoretically[10] or the contraction expected from Vegard's law based on a simple substitutional alloy. In addition, EXAFS data show increased disorder for the Pu-Pu near neighbor interactions. These results indicate that there are unexpected, site-specific lattice effects occurring in these materials.

The outline of the paper is as follows. Details of sample preparation and EXAFS experimental setup and data analysis are discussed in Sec. II. The results of curve-fitting analysis and modeling the temperature dependence using the correlated Debye model are presented in Sec. III. A discussion of the results and their relation to other Θ_D studies is presented in Sec. IV, and the conclusions are given in Sec. V.

II. EXPERIMENTAL DETAILS

A. Sample preparation

A ~ 6 μm thick ^{239}Pu foil (3.3 at.% Ga) was prepared from 20 year old material by melting to remove accumulated helium, followed by subsequent annealing, cutting, and rolling. The foil was further homogenized at 450 °C for ~ 100 h to ensure that single-phase, δ-Pu was produced. Transmission x-ray diffraction was performed at LLNL and confirmed the presence of the fcc phase, with no significant amounts of other Pu phases present. In preparation for EXAFS analysis, the foil was electropolished to remove any accumulated oxide material on the surface. The sample was then encapsulated under argon using a specially designed, triple containment x-ray compatible cell manufactured by Boyd Tech. The first level of containment consisted of coating the sample in a thin film of liquid polyimide solution that was allowed to air dry directly on the sample. The foil was then mounted onto an aluminum frame and sealed within two additional layers of x-ray transparent Kapton windows (0.010 in. thick). The windows were clamp mounted onto the aluminum body with stainless steel window frames and using indium wire as a vacuum seal material. The triple-contained sample was subsequently mounted in an open cycle liquid helium flow cryostat for variable temperature EXAFS measurements. Temperature measurement errors are within ~ 1 K, and are stable within ~ 0.2 K.

B. EXAFS data acquisition and analysis

Plutonium L_{III}- and gallium *K*-edge x-ray absorption spectra were collected at the Stanford Synchrotron Radiation Laboratory (SSRL) on wiggler beamline 11-2 under normal ring operating conditions using a nitrogen-cooled Si (220), half-tuned, double-crystal monochromator operating in unfocussed mode. The vertical slit height inside the x-ray hutch was 0.3 mm which reduces the effects of beam instabilities and monochromator glitches while providing ample photon flux. The Pu L_{III}-edge spectra were measured in transmission mode using Ar-filled ionization chambers. The Ga *K*-edge spectra were measured in fluorescence mode using a 30-element Ge array solid state detector developed by Canberra Industries. The detector was operated at ~ 75 kHz per channel, and the signals were digitally processed using the DXP 4C/4T developed by X-ray Instrumentation Associates.

XAFS raw data treatment, including calibration, normalization, and subsequent processing of the EXAFS and XANES (x-ray absorption near-edge structure) spectral regions was performed by standard methods reviewed elsewhere[20,21] using the EXAFSPAK suite of programs developed by G. George of SSRL. Typically, three XAFS scans (transmission or fluorescence) were collected from each sample at each temperature and the results were averaged. The spectra were energy calibrated by simultaneously measuring the absorption spectrum for the reference samples PuO_2 or Ga_2O_3. The energies of the first inflection points for the reference sample absorption edges E_r were defined at 18053.1 eV (Pu L_{III}) and 10368.2 eV (Ga *K*). The EXAFS threshold energies E_0 were defined as 18070 and 10 385 eV for the Pu and Ga edges, respectively. Nonlinear least-squares curve fitting was performed on the k^3-weighted EXAFS data using the EXAFSPAK programs.

The EXAFS data were fit using theoretical phase and amplitude functions calculated from the program FEFF8.1 of Rehr *et al.*[22,23] All of the Pu-Pu interactions were modeled using single scattering (SS) paths derived from the model compound, unalloyed δ-Pu, $a_{\mathrm{fcc}}=4.6371$ Å.[24] The Ga-Pu SS interactions were modeled by using the same model compound structure and replacing the central absorbing atom with Ga. An initial series of fits was done on the raw Pu L_{III} and Ga *K*-edge k^3-weighted data sets using the expected fcc near-neighbor interactions at 3.28, 4.64, 5.68, and 6.56 Å and fixing the coordination numbers at 12, 6, 24, 12, and 24, respectively. The results (especially at low *T*) confirmed the presence of the fcc structure and showed no evidence for other unusual structural effects. That is, we observed no phase changes (i.e., $\delta \rightarrow \alpha$) or previously postulated metastable impurity phases.[25,26] This first level of analysis was also used to establish values for S_0^2 and ΔE_0 by fixing coordination numbers *N* and allowing S_0^2, ΔE_0, σ^2, and *R* to vary. The final values used were taken from averaging over the range of temperatures studied: for Pu $S_0^2=0.55$, $\Delta E_0=-12$ eV and for Ga, $S_0^2=0.85$, $\Delta E_0=-10$ eV. The relatively low value of S_0^2 obtained for Pu in this alloy is close to the lower range of S_0^2 values reported for a wide variety of compounds.[21] However, due to the lack of reported S_0^2 values for Pu alloys in the literature, it is not clear whether this

value is anomalous or represents a real physical characteristic of the Pu atoms in this material. Forcing the fits to use a higher value of $S_0^2=0.9$ leads to extremely poor quality fits, particularly with respect to the EXAFS amplitude envelope.

As a result of the preliminary analyses, all of the subsequent fits described here focussed on isolating the behavior of the first shell Pu-Pu and Ga-Pu interactions in a highly constrained manner. Thus fits were done on Fourier-filtered data using the same fixed S_0^2 and ΔE_0 values for all temperatures, along with a fixed coordination number of $N=12$ for the first shell. The ability to fix ΔE_0, N, and S_0^2 helps to avoid correlation problems between the fit parameters and to establish more consistently any changes in σ^2 and R that may occur as functions of temperature.

III. RESULTS

A. EXAFS raw data and curve fitting

Figures 1(a) and 1(b) show the raw k^3-weighted Pu EXAFS L_{III} data and the corresponding Fourier transforms (FT) for the δ-Pu sample as a function of temperature. The FT represents a pseudoradial distribution function and the peaks are shifted to lower R values compared to real interaction values as a result of the phase shifts associated with the absorber-scatterer interactions ($\sim$0.1–0.2 Å for Pu-Pu). As the sample is cooled from 293 to 20 K, the EXAFS scattering amplitude increases systematically due to decreased thermal motion of the atoms in the lattice. As a result, the effective measurable k-range increases substantially at lower temperature. This effect is equally visible in the corresponding FT's. As the temperature is lowered, the intensity of the FT peaks increases dramatically, and the spectra reveal a pattern consistent with that expected for a fcc lattice. The first shell Pu-Pu peak seen at $\sim$3.1 Å corresponds to 12 Pu near neighbors in the fcc structure and increases in maximum peak height while also narrowing with decreasing temperature. The second, third, and fourth shell peaks at $\sim$4.4, 5.4, and 6.3 Å which correspond to real interactions at 4.64, 5.68, and 6.56 Å are clearly affected by thermal effects and become distinguishable only below 80 K.

The Ga K-edge raw k^3-weighted EXAFS and corresponding FT's are shown in Figs. 2(a) and 2(b). This series of spectra qualitatively exhibit the same thermal behavior observed in the Pu L_{III}-edge EXAFS data, that is, increased scattering amplitude along with detection of more distant neighbors are apparent with decreasing temperature. The spectra are dominated by the peak at $\sim$3.0 Å, attributed to the first shell Ga-Pu interactions ($N=12$). At lower temperatures, the FT's reveal second, third, and fourth shell Pu neighbor interactions at $\sim$4.4, 5.4, 6.3 Å, respectively. In contrast to the behavior observed in the Pu EXAFS, the detection of these longer range interactions is retained up to higher temperatures (around 110 K). At this level of analysis, this observation suggests that the Ga-Pu interactions experience less thermal broadening than the corresponding Pu-Pu interactions, which is especially surprising given the decreased reduced mass of the Ga-Pu pair relative to the Pu-Pu pair.

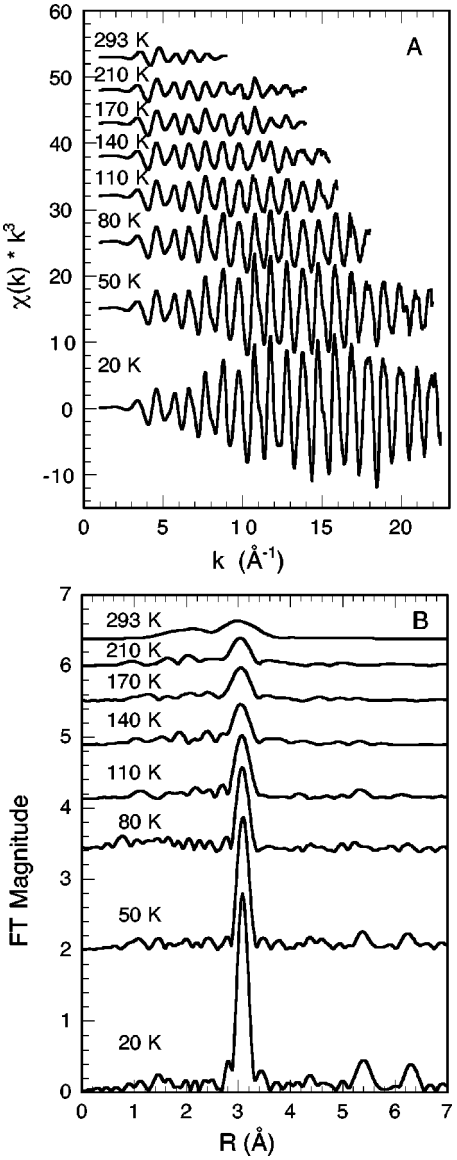

FIG. 1. Pu L_{III}-edge k^3-weighted EXAFS data (A) and the corresponding Fourier transforms (B) for the δ-Pu sample as a function temperature. Data were acquired in transmission mode and Fourier transformed over the ranges shown in the figure.

Following initial inspection of the data (see Sec. II) we chose to focus our analyses on the isolated first shell contributions, in part, due to the high signal-to-noise obtained relative to the more distant shell interactions. Thus by curve-fitting the Fourier-filtered first shell components from the Pu L_{III} and Ga K EXAFS, the local vibrational temperature dependence may be investigated. The first shell interactions were isolated by Fourier transforming over the data k ranges shown in Figs. 1(a) and 2(a), and back-transforming over the range $R=2-4$ Å.

The curve-fitting results summarized in Table I serve to identify the different temperature dependent and static structural effects for the Pu and Ga sites in this material. Figure 3 shows the resulting curve fits to the Fourier filtered Pu and Ga EXAFS data measured at 20 K in k and R space. The strong coincidence between the data and the fits serves to

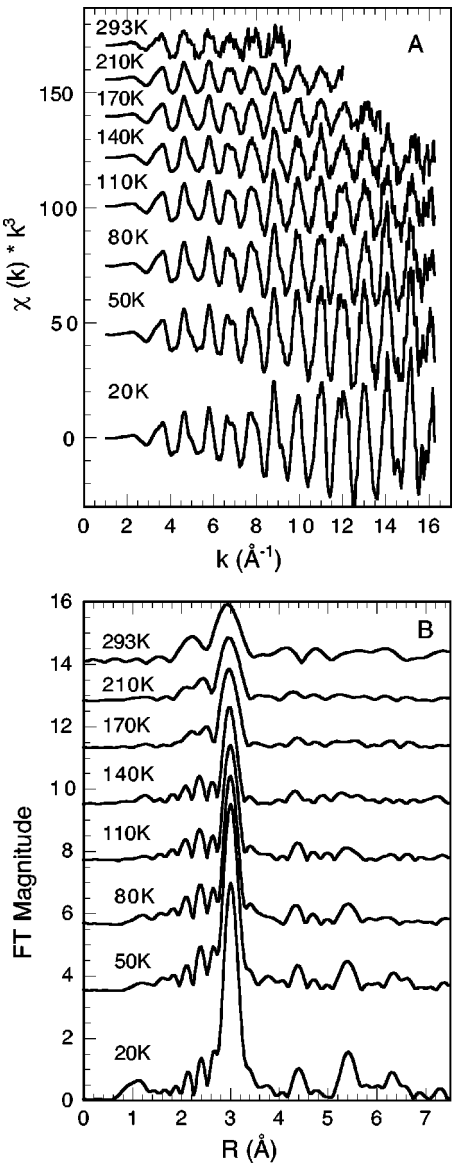

FIG. 2. Ga *K*-edge k^3-weighted EXAFS data (A) and the corresponding Fourier transforms (B) for the δ-Pu sample as a function temperature. Data were acquired in fluorescence mode and Fourier transformed over the ranges shown in the figure.

illustrate the highly refined nature of the FEFF8.1 calculations as well as the appropriateness of the fitting procedure employed. Because these fits were highly constrained, any changes in the data are assigned to changes in R and σ^2. The first effect revealed by these data is the overall contraction of Pu atoms around the Ga sites relative to the environment around the Pu sites. This ''collapse'' of about 4% is comparable to that observed by earlier EXAFS studies on δ-Pu.[17–19] The first shell bond lengths for each element appear to remain constant over the measured temperature range, at least within the quoted experimental error and under the constraints outlined above.

B. Vibrational analysis

The most dramatic effect depicted in this data set is the difference in the temperature dependence between the Pu-Pu and Ga-Pu Debye-Waller factors σ^2. The values for σ^2 increase with temperature consistent with greater thermal disorder, as expected. However, according to Table I, the Pu-Pu first shell shows much greater disorder at higher temperature than the corresponding Ga-Pu shell. Moreover, this occurs in

TABLE I. Pu L_{III} and Ga *K*-edge EXAFS single shell curve fitting results. The first shell interactions were isolated by Fourier transforming over the data k ranges displayed in Figs. 1(A) and 2(A), and back-transforming over the range $R=2-4$ Å. Several parameters were held fixed as follows: for Pu and Ga, $N=12$; for Pu, $S_0^2=0.55$ and $\Delta E_0=-12$ eV; and for Ga, $S_0^2=0.85$ and $\Delta E_0=-10$ eV.

Sample	Pu-Pu shell [a]		Ga-Pu shell	
Temp (K)	R (Å)	σ^2 (Å^2)	R (Å)	σ^2 (Å^2)
20	3.290	0.00280	3.160	0.00275
50	3.292	0.00381	3.160	0.00332
80	3.293	0.00511	3.160	0.00395
110	3.301	0.00680	3.160	0.00512
140	3.301	0.00905	3.160	0.00609
170	3.306	0.01039	3.163	0.00764
210	3.316	0.01275	3.165	0.00953
293	3.297	0.01821	3.171	0.01264

[a]Errors in R and σ^2 are estimated to be ± 0.005 Å and $\pm 10\%$ based on EXAFS fits to known model compounds, see Ref. 21.

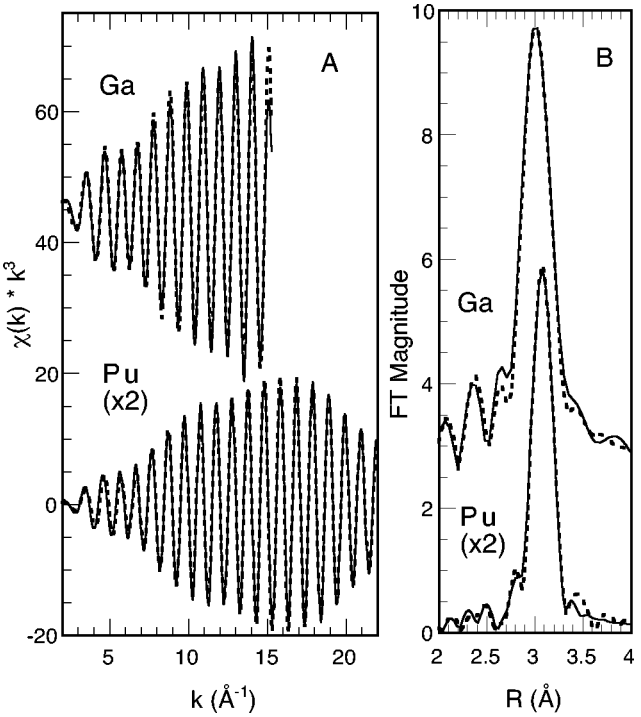

FIG. 3. Representative single shell curve fits (dotted lines) to the Pu L_{III} and Ga *K*-edge data (solid lines) measured at 20K in (A) *k*-space and (B) *R*-space. Data were Fourier-filtered from the raw spectra over the k and R ranges shown in the plots using Gaussian window functions with half-widths of 0.5 Å^{-1} and 0.05 Å, respectively. Pu data shown are multiplied by a factor of 2 for the purpose of comparison to the Ga data.

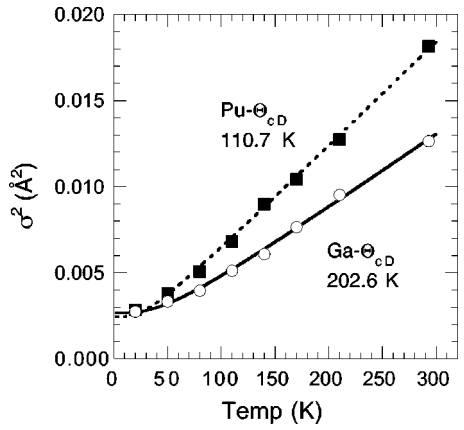

FIG. 4. Temperature dependence of EXAFS Debye-Waller factors for first shell Pu-Pu (upper data) and Ga-Pu (lower data) interactions plotted along with fits generated using the correlated Debye model.

spite of the fact that the Ga-Pu pair has a lower reduced mass. To study this effect more carefully, the temperature dependence of the Debye-Waller factors was modeled by employing the correlated-Debye model to determine the Debye temperature:[27]

$$\sigma^2_{\text{meas}}(T)=\sigma^2_{\text{static}}+F(T,\theta_{cD}). \tag{1}$$

The temperature-dependent part of the Debye-Waller factor $F(T,\theta_{cD})$ is given within the correlated-Debye model by

$$F(T,\theta_{cD})=\frac{\hbar}{2\mu}\int \rho_j(\omega)\text{cotanh}\left(\frac{\hbar\omega}{2k_BT}\right)\frac{d\omega}{\omega},$$

where μ is the reduced mass, θ_{cD} is the correlated Debye temperature, and the phonon density of states at position R_j is[28]

$$\rho_j=\frac{3\omega^2}{\omega_D^3}\left[1-\frac{\sin(\omega R_j/c)}{\omega R_j/c}\right] \tag{2}$$

in which ω_D is the usual Debye frequency and $c=\omega_D/k_B$ where k_B is Boltzmann's constant. The expression in brackets of Eq. (2) takes into account the correlated motion of the atom pairs.

Using this formalism, we obtain the fits shown in Fig. 4, and determine pair-specific correlated-Debye temperatures Θ_{cD} of 110.7 $\pm$1.7 K and 202.6$\pm$3.7 K, for the Pu and Ga sites, respectively. This analysis also estimates a value for $\sigma_{\text{static}}=0.02$ Å. Assuming that only 36% of the Pu atoms experience a direct Ga contraction, we can estimate the maximum static distortion by embedding a 0.12 Å contracted $GaPu_{12}$ cluster in an undistorted lattice and calculate the first shell distribution around the contracted Pu atoms. Using this approximation we obtain a maximum $\sigma_{\text{static}}=0.05$ Å. Although the expected distortion will be less due to further lattice relaxation, our value of 0.02 may indeed reflect additional relaxation and ordering around the Pu sites. The data appear to fit the model quite accurately, indicating that the local pair vibrations can be described using the correlated-Debye model. However, the higher Θ_{cD} of the Ga-Pu pair with respect to the Pu-Pu pair may indicate the presence of a local lattice anomaly from a vibrational standpoint, which could be related to the observed lattice contraction measured around the Ga sites.

TABLE II. Comparison of Pu and Ga specific Debye temperatures obtained for δ-Pu by various techniques.

δ-Pu alloy	Pu-Θ_D	Ga-Θ_D	Method
3.3 at. % Ga	110.7		EXAFS
		202.6	EXAFS
	127		neut. abs. [a]
		255	neut. abs.
	105		bulk mod. [b]
	115		elastic [c]
6.6 at. % Ga	127		elastic [d]
5.0 at. % Ga	132		elastic [e]
	132		neut. diff. [f]

[a]Neutron Resonance Doppler spectroscopy, Ref. 16.
[b]Using the relation from Ref. 31 and the experimental bulk modulus noted in the text.
[c]Ultrasonic measurement of 3 principal elastic constants C_{ij}, Ref. 14.
[d]Derived from Young's modulus, *E*, and torsional moduus, *G*, Ref. 29.
[e]Also derived from *E* and *G*, Ref. 30.
[f]Neutron diffraction, Ref. 15.

IV. DISCUSSION

It is instructive to compare the EXAFS Θ_{cD} results described here with those obtained from previous studies. Table II summarizes the Θ_D values for δ-Pu determined from our study along with those from earlier works. We also make special note of the differences in the methods used to determine these values, which is important for a proper interpretation. The elastic values of Θ_D are obtained by ultasound measurements of ''bulk'' lattice wave properties extrapolated down to $T=0$ K.[14,29,30] The ''bulk modulus'' value uses a theoretical relationship[31] where $\Theta_D=41.63\sqrt{r_0B/M}$ to derive Θ_D from an experimental value for $B=450$ kbar. The Θ_D value from neutron diffraction also represents a bulk measurement of lattice thermal behavior.[15] However, since it is derived from thermal displacement factors specifically attributed to the Pu atoms, it is referenced as Θ_{DW}. The Θ_D values obtained from EXAFS and neutron resonant absorption[16] are distinct from those derived from the other methods in that they are element specific, yet there are important differences to be noted. EXAFS inherently measures only phonon modes that involve specific atom pairs (i.e., we must consider the reduced mass for the pair). In contrast, neutron resonance absorption measures the average of all modes associated with a single atomic species (i.e., only the mass of the absorbing atom must be considered).

In general the Pu specific values of Θ_D obtained from all the techniques are similar in that they are all quite low, ranging from 104 to 132 K. It is not our intent to discuss these differences since they come from such a wide variety of

techniques and variability in samples. The Ga-specific Debye temperatures do, however, require more careful discussion, in relation to the Pu-specific values. As mentioned in Sec. I, neutron resonant absorption found a Ga specific Θ_D value of 255 K $\pm$22 K which, compared to the $\sqrt{m_{\mathrm{Pu}}/m_{\mathrm{Ga}}}$ weighted value of 236 K, does not exclude a slightly stiffer force field than the one around the Pu sites. Analogously, EXAFS yields a Ga specific Θ_{cD} of 202.6$\pm$3.7 K which may be compared to the expected value of 164 K (i.e., the $\sqrt{\mu_{\mathrm{Pu}}/\mu_{\mathrm{Ga}}}$ weighted value). The observation of a significantly higher Θ_{cD} for the Ga-Pu pair relative to that expected for a simple substitutional lattice model, coupled with the anomalously large lattice contraction around the Ga sites clearly suggest that the Ga sites reside in a significantly stronger force field. The shorter Ga-Pu bonds, in fact, inherently imply a strengthening of the Ga-Pu bonds relative to the Pu-Pu bonds.

Regarding factors that contribute to δ-phase stabilization, these results are consistent with the Ga atoms having a significant influence on the local electronic structure. One obvious possibility is that charge transfer exists between the Ga pd states and the corresponding Pu df states. In fact, a detailed model of hybridization was discussed in earlier work which measured the Ga *K*-edge XANES in a Pu-Ga alloy.[17] This orbital overlap will directly dictate the extent of lattice vibrational distortions and local geometry within the crystal structure, that is, with a preference towards a fcc lattice in the presence of Ga. Therefore, the results of this EXAFS study give evidence for the impact of the vibrational properties on the local lattice effects in the Pu-Ga alloy system. More work with other δ stabilizing elements is needed to determine if this is a universal characteristic applicable to all δ-phase stabilizers.

From the results of this study, we may also estimate values for ''pair-specific bulk moduli.'' Indeed, according to the empirical relation between bulk modulus and Debye temperature established by Moruzzi *et al.*,[31] we deduce from our calculated Debye temperatures for Pu and Ga values of 498 and 1666 kbar, respectively, for the bulk modulus. Since the Pu-Ga alloy we have been studying has a composition in the dilute limit, this implies that Pu is mostly surrounded by Pu atoms whereas each Ga site can be viewed as embedded in a Pu matrix. In addition, the bulk modulus of pure Ga metal as determined by theory,[32] 606 kbar, or experiment,[33] 613 kbar, is quite low in accordance with the low melting point of 308 K. Hence the dramatic difference between the two estimated bulk moduli provides an equivalent description for the increase in strength gained in going from Pu-Pu (or Ga-Ga bonds) to Ga-Pu bonds. This unusually large increase in stability of a Pu (Ga) matrix by addition of Ga (Pu) is reflected in the existence of very stable Pu-Ga compounds (i.e., large heats of formation), some of them exhibiting congruent melting. It would be interesting to extend this work to other alloy compositions to quantify more appropriately these findings and have a better understanding of the unusual synergistic effects due to alloying in Pu-Ga and related systems.

V. CONCLUSION

Pair specific Debye temperatures for the Ga-Pu and Pu-Pu pairs in δ-Pu were determined using a correlated-Debye model fit to temperature dependent EXAFS Debye-Waller parameters. Using this formalism, we obtain pair specific correlated-Debye temperatures Θ_{cD} of 110.7$\pm$1.7 K and 202.6$\pm$3.7 K, for the Pu-Pu and Ga-Pu pairs, respectively. The results for the Θ_{cD} Pu-Pu pair compare well with previous vibrational studies on δ-Pu. In addition, our results represent the first unambiguous determination of Ga-specific vibrational properties, i.e, Ga-Pu Θ_{cD}, in PuGa alloys. Because the Debye temperature can be related to a measure of the lattice stiffness, these results indicate that the Ga-Pu bonds experience a stronger force field than the corresponding Pu-Pu bonds. This effect has important implications for lattice stabilization mechanisms in these alloys. If the vibrational properties in δ-Pu are dependent on the type of impurity, further studies of Debye temperatures with other ''stabilizers'' will be important for discerning key aspects of the stabilization mechanism.

ACKNOWLEDGMENTS

This work was performed under the auspices of the U.S. Department of Energy (DOE) by the University of California Lawrence Livermore National Laboratory under Contract No. W-7405-Eng-48. This work was partially supported (C. H. B.) by the Office of Basic Energy Sciences, Chemical Sciences Division of the U. S. DOE, Contract No. DE-AC03-76SF00098. The authors also wish to thank John Rehr and Alex Ankudinov for helpful discussions. This work was done (partially) at SSRL, which is operated by the Department of Energy, Office of Basic Energy Sciences.

*Electronic address: allen42@llnl.gov

[1] W. N. Miner and F. W. Schonfeld, in *Plutonium Handbook*, edited by O. J. Wick (The American Nuclear Society, La Grange Park, IL, 1990), p. 33.

[2] J. L. Smith and E. A. Kmetko, J. Less-Common Met. **90**, 83 (1983).

[3] J. M. Willis and O. Eriksson, Phys. Rev. B **45**, 13 879 (1992).

[4] P. Chiotti, V. V. Akhachinskij, I. Ansara, and M. H. Rand, *The Chemical Thermodynamics of Actinide Elements and Compounds (The American Nuclear Society, International Atomic Energy Agency, Vienna, 1981)*, Vol. 5, p. 231.

[5] P. H. Adler, G. B. Olson, M. F. Stevens, and G. F. Gallegos, Acta Metall. Mater. **40**, 1073 (1992).

[6] T. G. Zocco, M. F. Stevens, P. H. Adler, R. I. Sheldon, and G. B. Olson, Acta Metall. Mater. **38**, 2275 (1990)

[7] J. R. K. Gschneidener, R. O. Elliott, and V. O. Struebing, in *Plutonium 1960* (Cleaver-Hume, London, 1961), p. 99.

[8] P. H. Adler, Metall. Trans. A **22**, 2237 (1991).

[9] P. Weinberger, A. M. Boring, and J. Smith, Phys. Rev. B **31**, 1964 (1985).

[10] J. D. Becker, J. M. Wills, L. Cox, and B. R. Cooper, Phys. Rev. B **58**, 5143 (1998).

[11] P. E. A. Turchi, A. Gonis, N. Kioussis, D. L. Price, and B. R.

Cooper, in *Proceedings of the International Workshop on Electron Correlations and Materials Properties*, edited by A. Gonis, N. Kioussis, and M. Ciftan (Kluwer Academic, New York, 1999), pp. 531–537.
[12] M. Pénicaud, J. Phys.: Condens. Matter **9**, 6341 (1997).
[13] S. Méot-Reymond and J. M. Fournier, J. Alloys Compd. **232**, 119 (1996).
[14] H. M. Ledbetter and R. M. Moment, Acta Metall. **24**, 891 (1976).
[15] A. Lawson, J. Goldstone, B. Cort, R. Sheldon, and E. Folyton, J. Alloys Compd. **213**, 426 (1994).
[16] J. Lynn, G. Kwei, W. J. Trela, V. W. Yuan, B. Cort, R. J. Martinez, and F. Vigil, Phys. Rev. B **58**, 11 408 (1998).
[17] L. Cox, R. Martinez, J. H. Nickel, S. Conradson, and P. Allen, Phys. Rev. B **51**, 751 (1995).
[18] P. Faure, B. Deslandes, D. Bazin, C. Tailland, R. Doukhan, J. M. Fournier, and A. Falanga, J. Alloys Compd. **244**, 131 (1996).
[19] N. Richard, P. Faure, P. Rofidal, J. L. Truffier, and D. Bazin, J. Alloys Compd. **2711-273**, 879 (1998).
[20] T. M. Hayes and J. B. Boyce, in *Solid State Physics*, edited by H. Ehrenreich, F. Seitz, and D. Turnbull (Academic, New York, (1982), Vol. 37, p. 173.
[21] G. G. Li, F. Bridges, and C. H. Booth, Phys. Rev. B **52**, 6332 (1995).
[22] J. J. Rehr, J. Mustre de Leon, S. I. Zabinsky, and R. C. Albers, Phys. Rev. B **44**, 4146 (1991).
[23] J. J. Rehr, J. Mustre de Leon, S. I. Zabinsky, and R. C. Albers, J. Am. Chem. Soc. **113**, 5135 (1991).
[24] F. H. Ellinger, J. Met. **8**, 1256 (1956).
[25] S. D. Conradson, Appl. Spectrosc. **52**, 252A (1998).
[26] S. D. Conradson (unpublished).
[27] E. D. Crozier, J. J. Rehr, and R. Ingalls, in *X-Ray Absorption: Principles, Applications, Techniques of EXAFS, SEXAFS, XANES*, edited by D. Konigsberger and R. Prins (Wiley, New York, 1988), p. 373.
[28] G. B. Beni and P. M. Platzman, Phys. Rev. B **14**, 1514 (1976).
[29] J. C. Taylor, P. F. T. Linford, and D. J. Dean, J. Inst. Met. **96**, 178 (1968).
[30] M. Rosen, G. Frez, and S. Shtrikman, J. Phys. Chem. Solids **30**, 1063 (1969).
[31] V. L. Moruzzi, J. F. Janak, and K. Schwarz, Phys. Rev. B **37**, 790 (1988).
[32] P. E. A. Turchi, A. Gonis, and N. Kioussis calculated for hypothetical fcc-based Ga using the full-Potential linear muffin-tin orbital method (unpublished).
[33] R. W. G. Wyckoff, *Crystal Structures*, 2nd ed. (Wiley, New York, 1962), Vol. 1, p. 22.